RESEARCH ARTICLE

Proportional Accumulation of Yolk Proteins Derived From Multiple Vitellogenins is Precisely Regulated During Vitellogenesis in Striped Bass (*Morone saxatilis*)

JOURNAL OF EXPERIMENTAL ZOOLOGY
PART A
ECOLOGICAL GENETICS AND PHYSIOLOGY
A Journal of Integrative Biology

VALERIE N. WILLIAMS[1], BENJAMIN J. READING[1]*, HARUNA AMANO[2], NAOSHI HIRAMATSU[2], JUSTIN SCHILLING[1], SCOTT A. SALGER[1], TAUFIKA ISLAM WILLIAMS[3], KEVIN GROSS[4], AND CRAIG V. SULLIVAN[1]

[1]Department of Applied Ecology, College of Agriculture and Life Sciences of North Carolina State University, Raleigh, North Carolina
[2]Graduate School of Fisheries Sciences, Hokkaido University, Hakodate, Hokkaido, Japan
[3]Mass Spectrometry Laboratory, College of Agriculture and Life Sciences of North Carolina State University, Raleigh, North Carolina
[4]Department of Statistics, North Carolina State University, Raleigh, North Carolina

ABSTRACT

We quantified three vitellogenins (VtgAa, VtgAb, VtgC) or their derived yolk proteins (YPs) in the liver, plasma, and ovary during pre-vitellogenic (PreVG), mid-vitellogenic (MVG), and late-vitellogenic (LVG) oocyte growth and during post-vitellogenesis (PostVG) in the striped bass (*Morone saxatilis*) using label-free quantitative mass spectrometry (MS). Western blotting of the samples using antisera raised against gray mullet (*Mugil cephalus*) lipovitellins derived from VtgAa, VtgAb, and VtgC confirmed the MS results. Semi-quantitative reverse transcription polymerase chain reaction (RT-PCR) revealed liver as the primary site of expression for all three Vtgs, with extra-hepatic transcription weakly detected in ovary, foregut, adipose tissue, and brain. Quantitative real-time RT-PCR confirmed *vtgAb* to be primarily expressed in liver and VtgAb proteins were predominant in liver and plasma from MVG to PostVG. However, the primary period of deposition into oocytes of VtgAb occurred up until MVG, whereas VtgAa was primarily deposited from MVG to LVG. The VtgC was gradually taken up by oocytes throughout vitellogenesis and was detected at trace levels in plasma. The ratio of yolk proteins derived from VtgAa, VtgAb, VtgC (YPAa/YPAb/YPC) in PostVG ovary is 1.4:1.4:1, which differs from ratios previously reported for other fish species in that YPC comprises a greater proportion of the egg yolk. Our results indicate that proportional accumulation of multiple Vtgs in the yolk may depend both on the precise rates of their hepatic secretion and specific uptake by oocytes. Furthermore, composition of the Vtg-derived yolk may vary among Acanthomorph fishes, perhaps reflecting their different early life histories and reproductive strategies. *J. Exp. Zool. 321A:301–315, 2014.* © 2014 Wiley Periodicals, Inc.

How to cite this article: Williams VN, Reading BJ, Amano H, Hiramatsu N, Schilling J, Salger SA, Islam Williams T, Gross K, Sullivan CV. 2014. Proportional accumulation of yolk proteins derived from multiple vitellogenins is precisely regulated during vitellogenesis in striped bass (*Morone saxatilis*). J. Exp. Zool. 321A:301–315.

J. Exp. Zool. 321A:301–315, 2014

Vitellogenins (Vtgs), the major precursors of egg yolk proteins (YPs), are typically synthesized in the liver and secreted into the bloodstream following induction by estrogen during the main phase of ovarian growth, termed *vitellogenesis*. Circulating Vtgs are taken up specifically by growing oocytes, where they are proteolytically processed into a characteristic suite of derivative YPs, including lipovitellin (Lv), phosvitin (Pv), beta'-component (β′-c), C-terminal peptide (C-t), and various Lv–Pv complexes. These YPs are then stored in the ooplasm to later serve crucial functions in both the physiology of ovulated eggs and the nutrition of developing embryos and larvae (review: Hiramatsu et al., 2005, 2006; Reading et al., 2009; Reading and Sullivan, 2011).

Multiplicity of Vtgs has been reported in several species of fishes: mummichog (*Fundulus heteroclitus*; LaFleur et al., '95, 2005), barfin flounder (*Verasper moseri*; Matsubara et al., '99), haddock (*Melanogrammus aeglefimus*; Reith et al., 2001), zebrafish (*Danio rerio*; Wang et al., 2000, 2005), mosquitofish (*Gambusia affinis*; Sawaguchi et al., 2005a,b), red seabream (*Pagrus major*; Sawaguchi et al., 2006), Atlantic halibut (*Hippoglossus hippoglossus*; Finn, 2007a,b), gray mullet (*Mugil cephalus*; Amano et al., 2007a), white perch (*Morone americana*; Hiramatsu et al., 2002b; Reading et al., 2009), and goldsinny wrasse (*Ctenolabrus rupestris*; Kolarevic et al., 2008). In advanced teleosts (Acanthomorpha), complete Vtgs can be classified based upon their structures and functions as either VtgAa or VtgAb type according to the nomenclature proposed by Finn and Kristofferson (2007). During ovarian maturation in marine species that spawn pelagic eggs, the major subunit of Lv (LvH) derived from VtgAa (LvHAa) undergoes proteolysis into free amino acids (FAAs), whereas the LvH from VtgAb (LvHAb) largely survives this degradation (Matsubara et al., '99; Reith et al., 2001; Finn, 2007a). The FAAs derived from VtgAa generate an osmotic gradient, which promotes oocyte hydration, resulting in appropriately buoyant eggs (Matsubara et al., '99). Additionally, FAAs are used as diffusible nutrients to support early embryogenesis, whereas intact LvHAb is consumed by later stage embryos and larvae (Matsubara et al., '99; Sawaguchi et al., 2005b, 2006; Amano et al., 2007a,b, 2008).

A third type of incomplete Vtg that lacks or has truncated Pv, β′-c, and C-t domains is classified as VtgC (Wang et al., 2000; Finn and Kristofferson, 2007). The VtgC may supply nutrients to developing yolk sac larvae (Sawaguchi et al., 2005b) without influencing oocyte hydration or egg buoyancy (Reading and Sullivan, 2011). This current paradigm of teleost vitellogenesis based on Vtg multiplicity is further complicated by the recent report of multiple ovarian Vtg receptors (Vtgrs) that disparately bind to the Vtg yolk precursors (Reading et al., 2011; Hiramatsu et al., 2013).

We recently reported the full-length striped bass *vtgAa*, *vtgAb*, and *vtgC* gene transcripts and characterized their derivative YP products in striped bass oocytes and eggs (Williams et al., 2014). Although the striped bass has a multiple Vtg system, these different Vtgs have not yet been quantified during different phases of the female reproductive cycle. Tao et al. ('93) is the only previous report of Vtg quantification in female striped bass plasma, however, these data likely represent measurement of what we now consider to be a mixture of VtgAa and VtgAb. Understanding the profiles of VtgAa, VtgAb, and VtgC content by tissues that are directly involved in vitellogenesis would advance our understanding of how oocytes specifically and proportionally accumulate Vtg-derived YPs (YPAa, YPAb, and YPC, respectively) that later serve critical functions during ovarian maturation and early ontogeny.

Quantification of the three Vtg protein levels is challenging, since methods that require type-specific antisera, such as enzyme-linked immunosorbent assay (ELISA), are commonly employed for this purpose. Obtaining preparations of the different forms of Vtg that are sufficiently purified for use as antigens to develop Vtg-type-specific antisera is technically very difficult to achieve and thus far has been accomplished for only three species: gray mullet (Amano et al., 2007a,b, 2008), barfin flounder (Sawaguchi et al., 2008), and recently white perch (Williams et al., 2014). Therefore, we used a label-free quantitative mass spectrometry (MS) technique to simultaneously measure, for the first time, the abundance of multiple Vtgs in the liver and blood plasma, and of their derivative YPs in the ovary of female striped bass during pre-vitellogenesis (PreVG), mid-vitellogenesis (MVG), late vitellogenesis (LVG), and post-vitellogenesis (PostVG). Western blots employing Vtg-type-specific polyclonal antisera raised against the corresponding gray mullet Lvs were performed for samples of striped bass liver, plasma, and ovary and were used to confirm the MS findings. Additionally, we report on expression of the different *vtg* genes in seven different tissues of female striped bass during MVG and in liver and ovary during PreVG, MVG, LVG, and PostVG.

MATERIALS AND METHODS

Sample Collection

Female striped bass ($N = 12$) from the North Carolina State University Pamlico Aquaculture Field Laboratory (NCSU PAFL) were sampled for plasma, liver, and ovary at four time points throughout an annual reproductive cycle ($N =$ three fish per time

Conflicts of interest:None.
Craig V. Sullivan's current address: Craig V. Sullivan, Carolina AquaGyn, P.O. Box 12914, Raleigh, NC 27605
*Correspondence to: Benjamin J. Reading, Department of Applied Ecology, North Carolina State University, 127 David Clark Labs, Raleigh, NC 27695.
E-mail: bjreadin@ncsu.edu
Received 12 September 2013; Revised 7 February 2014; Accepted 20 February 2014
DOI: 10.1002/jez.1859
Published online 20 March 2014 in Wiley Online Library (wileyonlinelibrary.com).

point, all values are given as mean ± standard error of the mean): August (body weight 1.90 ± 0.35 kg; total length 512 ± 10.4 mm), November (3.80 ± 0.08 kg; 625 ± 3.45 mm), February (4.40 ± 0.54 kg; 626 ± 27 mm), and April (4.54 ± 0.79 kg; 663 ± 43 mm). All animals were treated according to the Guide for Care and Use of Laboratory Animals (National Research Council, '96). Females were anesthetized with Finquel MS-222 (Argent Chemical Laboratories, Redmond, WA, USA) and ovary biopsies were sampled using a plastic cannula inserted through the urogenital pore (Rees and Harrell, '90). Maximum oocyte diameters were measured under a dissecting stereomicroscope fitted with a calibrated ocular micrometer. The stage of ovarian development was determined by the maximum diameter of oocytes in the August, November, February, and April biopsy samples based on Berlinsky and Specker ('91) as follows: PreVG (310 ± 12.6 μm), MVG (503 ± 34.7 μm), LVG (831 ± 160 μm), or PostVG (986 ± 19.1 μm), respectively. Blood was sampled from the caudal peduncle and plasma was collected following centrifugation for 10 min at 25°C; plasma collected for Western blotting was treated with one TIU/mL aprotinin (Heppell et al., '99). Females were euthanized with Finquel MS-222 and liver and ovary tissues were dissected and flash frozen in liquid nitrogen. Plasma samples were stored at −20°C and ovary and liver samples were stored at −80°C until being submitted to analysis by MS and Western blotting. Liver and ovary tissues also were preserved in RNALater (Ambion, Grand Island, NY, USA) and stored at −20°C until use to prepare templates for quantitative RT-PCR.

Female striped bass (N = three) were sampled during MVG (body weight 2.89 kg ± standard error of the mean 0.28 kg; total length 422.45 mm ± standard error of the mean 84.44 mm, maximum oocyte diameter 508.33 μm ± standard error of the mean 13.87 μm) for brain, heart, liver, ovary, gut, muscle, and adipose tissues as described above. Tissues were preserved in RNALater and stored at −20°C until used to prepare templates for semi-quantitative RT-PCR.

Quantitative Mass Spectrometry

Plasma samples were diluted to a protein concentration of 0.50 μg/μL in MilliQ water (EMD Millipore Corporation, Billerica, MA, USA) measured using a NanoDrop ND-1000 (OD_{280}) (Thermo, San Jose, CA, USA). Ovary and liver tissues were homogenized 1:4 (w/v) in MilliQ ultrapure water. Extracts were centrifuged for 10 min at 13,000 rpm and 4°C and supernatants diluted to 0.50 μg/μL as described above. Samples were subjected to trypsin digest and reversed phase HPLC separation and tandem mass spectrometry (nano-LC-MS/MS) at the North Carolina State University Mass Spectrometry Facility (Raleigh, NC, USA) as described in Reading et al. (2013). The nano-LC-MS/MS was performed using an Eksigent (Dublin, CA, USA) nano-LC-1D+ system with an autosampler coupled to a hybrid LTQ-Orbitrap XL mass spectrometer (Thermo Scientific). All samples were measured in triplicate.

Data files were processed by MASCOT (Matrix Science, Boston, MA, USA) for protein identifications. Both MS and MS/MS data were interrogated. Batch searching of nano-LC-MS/MS data was performed using the three-spined stickleback (*Gasterosteus aculeatus*) protein database from ENSEMBL downloaded on March 17, 2011 from the ENSEMBL website and manually modified to also include protein sequences for striped bass VtgAa, VtgAb, and VtgC, *H. sapiens* keratin, and porcine trypsin. A Perl script was used to create a reverse modified stickleback protein database. All sequences were combined into one FASTA file for MASCOT searching of nano-LC-MS/MS data to account for the false discovery rate (FDR). An FDR of <1% is considered adequate and was used in determining reliable protein identifications. The following variable and fixed amino acid modifications were allowed in all of the database searches: variable methionine (M) oxidation, asparagine (N), and glutamate (Q) deamidation, fixed cystine carbamindomethylation. The MASCOT search parameters were as follows: maximum missed cleavages 2, peptide charge 1+, 2+, and 3+, peptide tolerance ±5 ppm, and MS/MS tolerance ± 0.6 Da.

Spectral counts for each identified protein were normalized to total spectral counts from MASCOT for each replicate using ProteoIQ (v. 2.3.01; NuSep, Bogart, GA, USA). Shared peptides were apportioned among protein groups (Zhang et al., 2010) and normalized to protein length (NSAF; Zybailov et al., 2006, 2007). The normalized spectral counts (NSC) for each of the three technical replicates per biological sample were exported from ProteoIQ and transformed to stabilize the variance [$\log_{10}(y+1)$, where y = NSC]. Data were analyzed by analysis of variance (ANOVA) using two methods (SAS v. 9.2; Cary, NC, USA): (1) A mixed-effects ANOVA with a fixed effect for differences among the Vtgs and a random blocking factor for differences among individual fish. The Tukey–Kramer Honestly Significant Difference (HSD) was used as a post hoc test for comparisons of Vtg-type by tissue (liver, plasma, and ovary) using $\alpha = 0.05$ as the nominal level of significance. (2) A one-way ANOVA for analyzing transformed NSC changes by Vtg-type across time. The Tukey–Kramer HSD was used as a post hoc test for comparisons of Vtg-type by time (PreVG, MVG, LVG, PostVG) using $\alpha = 0.05$ as the nominal level of significance.

Polyacrylamide Gel Electrophoresis (SDS–PAGE) and Western Blotting

Liver and ovary were homogenized on ice at 1:4 w/v in MilliQ ultrapurified water containing aprotinin (one TIU/mL) with a hand held tissue homogenizer (Dremel Multipro, Mount Prospect, IL, USA) using two bursts for 30 sec. Estrogen-induced and normal male plasma (negative control) was obtained from striped bass and prepared for Western blotting according to Williams et al. (2014) (see also: Tao et al., '93). White perch VtgAa, VtgAb, and VtgC were purified from the plasma of E_2-induced male fish by column chromatography as described in Reading et al. (2011).

Homogenates and plasmas were centrifuged at 13,000*g* for 10 min at 4°C and protein concentrations of the supernatants were measured by NanoDrop ND-1000. Samples were combined equally by total protein from $N =$ three individuals for each time point and diluted 1:1 with Laemmli buffer containing β-mercaptoethanol (Laemmli, '70). Samples were boiled for 5 min and loaded equally by protein concentration on 4–15% Tris–HCl ReadyGels (BioRad, Hercules, CA, USA) for SDS–PAGE. Gels were stained with 0.1% Coomassie brilliant blue R250 (CBB) in a solution of ethanol/acetic acid/distilled water (4:1:5 v/v; CBB stain) and destained in a solution of methanol/acetic acid/distilled water (3:1:6 v/v) or electro-blotted to PVDF membranes for Western blotting using three polyclonal antisera raised against gray mullet Lvs that were purified from oocyte extracts (Amano et al., 2007a,b, 2008). These antisera, α-Mullet LvAa, α-Mullet LvAb, and α-Mullet LvC, correspond to VtgAa, VtgAb, and VtgC, respectively, and were used in Western blotting at final concentrations of 1:40,000 (v/v), 1:260,000 (v/v), and 1:20,000 (v/v), respectively. Gels were calibrated with SDS–PAGE standards (BioRad) and the molecular weight of each protein band was calculated using the GeneGenius scanner and GeneTools software (Syngene, Fredrick, MD, USA).

Semi-Quantitative Reverse Transcription Polymerase Chain Reaction (RT-PCR)

Total RNA was purified using Trizol Reagent (Invitrogen, Grand Island, NY, USA) and RNA quality was evaluated by OD_{260}/OD_{280} and OD_{260}/OD_{230} using a NanoDrop ND-1000 spectrophotometer and agarose gel electrophoresis. Acceptable RNA extractions (OD ratios = 1.8–2.0 with good ribosomal RNA integrity) were treated with Turbo DNA-free (Ambion, Foster City, CA, USA) and cDNA was synthesized using the Superscript First Strand Synthesis System (Invitrogen) with a mixture of random hexamers and oligo-dTs as described by the manufacturer. Specific PCR primers were designed based on striped bass *vtgAa* (F-5′-CGCCAAAATCACAGCAAGAC-3′; R-5′-GACCAACTATCAGCAACCGATG-3′), *vtgAb* (F-5′-TTCTAAAAA TCCACGAGGCTC-3′; R-5′-AGCATCCAACACCCTTCTGC-3′), and *vtgC* (F-5′-TTCAAAGTAGTCCCAGCC-3′; R-5′-TCCAGCCTTCCAT-TAGGTG-3′) cDNA sequences (Williams et al., 2014; GenBank accession numbers: HQ846509, HQ846510, HQ846511, respectively) and 60s ribosomal protein L9 (F-5′-ATGAGGACTGGTGTGAACTGT-3′; R-5′-CGCTCTATGAGTGCTGTGGTAA-3′), *rpl9* (contig 10830; Reading et al., 2012). The *rpl9* was chosen as an internal reference gene based on its performance reported by Jonge et al. (2007) and Geist et al. (2007).

Polymerase chain reaction was performed using Platinum PCR SuperMix (Invitrogen) with each tissue cDNA as template following the protocol provided by the manufacturer. The following thermal parameters were used: 94°C for 2 min (initial denaturing) and 20–35 cycles at 94°C for 30 sec (denaturing), 54°C for 30 sec (annealing), and 68°C for 30 sec (extension), with a final extension at 72°C for 7 min. Amplicons and DNA size markers (Sigma, St. Louis, MO, USA) were separated by electrophoresis through a 0.9% agarose gel containing 1 μg/μL ethidium bromide and gels were visualized on a UV transilluminator using the GeneGenius scanner and GeneTools software (Syngene).

Real-Time Quantitative RT-PCR

Total RNA from female striped bass liver and ovary sampled at PreVG, MVG, LVG, and PostVG was isolated using TRIzol Reagent (Invitrogen). The RNA quality was evaluated by OD_{260}/OD_{280} and OD_{260}/OD_{230} using a NanoDrop ND-1000 spectrophotometer and agarose gel electrophoresis. Acceptable RNA extractions (OD ratios = 1.8–2.0 with good ribosomal RNA integrity) were treated with Turbo DNA-free (Ambion, Foster City, CA, USA) and cDNA was synthesized with a High Capacity cDNA Synthesis Kit (Applied Biosystems, Carlsbad, CA, USA). Specific primers for striped bass *vtgAa* (F-5′-AAACAGCAGAAGCCCACCT-3′ and R-5′-TCGCCATAATTGAAACAACTTT-3′), *vtgAb* (F-5′-TGAGGGT-CTGACCAGCATCT-3′ and R-5′-CATGAGTTAAGGCAATGGGA-TT-3′), and *vtgC* (F-5′-CAACAATGGACAGCTTTGGA-3′ and R-5′-GGTGGTGAGATTTTGGTTGC-3′) were designed from the full-length cDNA sequences reported in Williams et al. (2014) using MacVector (Cary, NC, USA). These primers amplified 149, 114, and 110 bp products corresponding to *vtgAa*, *vtgAb*, and *vtgC*, respectively.

Picha et al. (2006) show that normalization of target RNA to total RNA in the liver of hybrid striped bass yields results similar to that for normalization to 18S RNA. Therefore, we used total RNA for normalization of *vtg* gene expression by tissue at a specific time point in absolute quantitative real-time RT-PCR and we used *rpl9* as an internal reference gene for normalization of liver *vtg* gene expression across time in relative quantitative real-time RT-PCR as follows.

Absolute quantitative real-time RT-PCR assays of striped bass *vtgAa*, *vtgAb*, and *vtgC* gene expression were designed based on Tipsmark et al. (2008) using Brilliant II SYBR Green QPCR Master Mix (Agilent Technologies, Clara, CA, USA). No template controls and no reverse transcription controls were incorporated into each assay. All samples were measured in triplicate wells using a 7300 Real Time PCR System (Applied Biosystems) and the following thermal parameters: one cycle, 95°C for 10 min; 40 cycles, 95°C for 30 sec, 60°C for 1 min. Pooled cDNA samples were used to normalize data between plates. Gene expression was reported as copy number/ng of total RNA calculated by dividing the anti-log of copy number predicted from mean cycle thresholds of serially diluted plasmid DNA standard curves by the normalized total RNA concentrations (Nolan et al., 2006). Melting curve analysis and agarose gel electrophoresis were performed to verify primer specificity. Data were analyzed using mixed-effects ANOVA with a fixed effect for differences among the *vtgs* and a random blocking factor for differences among individual fish. The Tukey–Kramer HSD was used as a post hoc test for comparisons of Vtg-type by tissue (liver and ovary) using $\alpha = 0.05$ as the nominal level of significance.

Relative quantitative real-time RT-PCR was performed using *rpl9* (F-5′-TCAAGGGAGTCACTTTGGGTTTC-3′ and R-5′GACACCAGCTCAATGTCGTTACC-3′) as an internal reference gene and the same cDNA templates (PreVG, MVG, LVG, and PostVG) and *vtg* primers as described above. Gene expression was normalized against the reference gene and quantified using the $\Delta\Delta C_t$ method (Nolan et al., 2006; Davis et al., 2007). Data ($\Delta\Delta C_t$ fold change) were analyzed by a one-way ANOVA and the Tukey–Kramer HSD was used as a post hoc test for comparisons of *vtg*-type across time (PreVG, MVG, LVG, PostVG) using $\alpha = 0.05$ as the nominal level of significance.

RESULTS

Quantitative Mass Spectrometry

Label-free quantitative MS data for multiple Vtgs and their derivative YPs present in liver, plasma, and ovary of striped bass during PreVG, MVG, LVG, and PostVG are provided in Supplemental Table S1. Average NSC values for peptides attributable each type of striped bass Vtg that were detected in the liver, plasma, and ovary at these ovarian stages are reported in Table 1, and these data are graphically represented in Figure 1. The three Vtgs either were not detected or present at trace levels in all sample types during PreVG. The VtgAb NSC was significantly higher than that for VtgAa and VtgC in the liver during MVG and PostVG. The VtgAa and VtgAb NSC values were both significantly higher than the NSC for VtgC in liver during LVG. The VtgAb NSC was significantly higher than that for either VtgAa or VtgC in the plasma during MVG and PostVG. The VtgAa NSC was also significantly higher than that for VtgC in the plasma during LVG.

The NSC for VtgAa in liver significantly increased from PreVG to LVG ($P = 0.004$), MVG to LVG ($P = 0.006$), and LVG to PostVG ($P = 0.044$). The NSC for VtgAb in liver significantly increased from PreVG to MVG ($P = 0.0004$), PreVG to LVG ($P = 0.0001$), and PreVG to PostVG ($P = 0.0001$). The VtgC was not detected in liver at any stage. The NSC for VtgAa in plasma significantly increased from PreVG to LVG ($P = 0.006$) and from MVG to LVG ($P = 0.032$). The NSC for VtgAb in plasma significantly increased from PreVG to MVG ($P = 0.0001$), PreVG to LVG ($P = 0.0001$), PreVG to PostVG ($P = 0.0001$), and from MVG to LVG ($P = 0.040$). The VtgC was either detected in plasma at trace levels or was not detected at any ovarian stage. The NSCs for VtgAa and for VtgAb were significantly ($P = 0.05$) higher than that for VtgC in ovary during LVG and PostVG. The NSC values for VtgAa, VtgAb, and VtgC in ovary significantly increased from PreVG to MVG ($P = 0.0002$, $P = 0.0001$, and $P = 0.0001$, respectively), from PreVG to LVG ($P = 0.0001$, $P = 0.0001$, and $P = 0.0001$, respectively), and from PreVG to PostVG ($P = 0.0001$, $P = 0.0001$, and $P = 0.0001$, respectively). The NSC for VtgC in ovary also significantly increased from MVG to PostVG ($P = 0.029$).

The proportional abundance of striped bass Vtgs (VtgAa/VtgAb/VtgC) or of their product YPs in each sample type at the

Table 1. Average normalized spectral count (NSC) values for each vitellogenin (VtgAa, VtgAb, and VtgC) identified in liver, plasma, and ovary of striped bass during PreVG, MVG, LVG, and PostVG.

	VtgAa	VtgAb	VtgC	VtgAa/VtgAb/VtgC
Liver				
PreVG	0	0	0	0:0:0
MVG	0.04 ± 0.139	6.01 ± 0.121	0	1:126.8:0
LVG	4.33 ± 0.102	13.48 ± 0.102	0	1:3.12:0
PostVG	0.95 ± 0.098	13.48 ± 0.098	0	1:14.3:0
Plasma				
PreVG	0	0	0.36 ± 0.016	0:0:1
MVG	0.75 ± 0.103	7.60 ± 0.103	0.22 ± 0.103	1:10.12:0
LVG	5.80 ± 0.102	14.50 ± 0.102	0	1:2.5:0
PostVG	1.53 ± 0.160	11.52 ± 0.160	0.46 ± 0.160	3.35:25.2:1
Ovary				
PreVG	0.15 ± 0.040	0.08 ± 0.040	0	1.9:1:0
MVG	22.44 ± 0.166	53.14 ± 0.166	21.35 ± 0.166	1.05:2.5:1
LVG	53.84 ± 0.069	53.83 ± 0.069	27.41 ± 0.069	1.9:1.9:1
PostVG	56.46 ± 0.030	55.53 ± 0.030	39.61 ± 0.030	1.43:1.40:1

The proportional Vtg abundance (VtgAa/VtgAb/VtgC) is reported as a ratio of NSC values. The mean ± standard error of the mean value is reported (see text for details).
LVG, late-vitellogenesis; MVG, mid-vitellogenesis; NSC, normalized spectral counts; PostVG, post-vitellogenesis; PreVG, pre-vitellogenesis; VtgAa/VtgAb/VtgC, proportional Vtg abundance; VtgAa, VtgAb, and VtgC, vitellogenins.

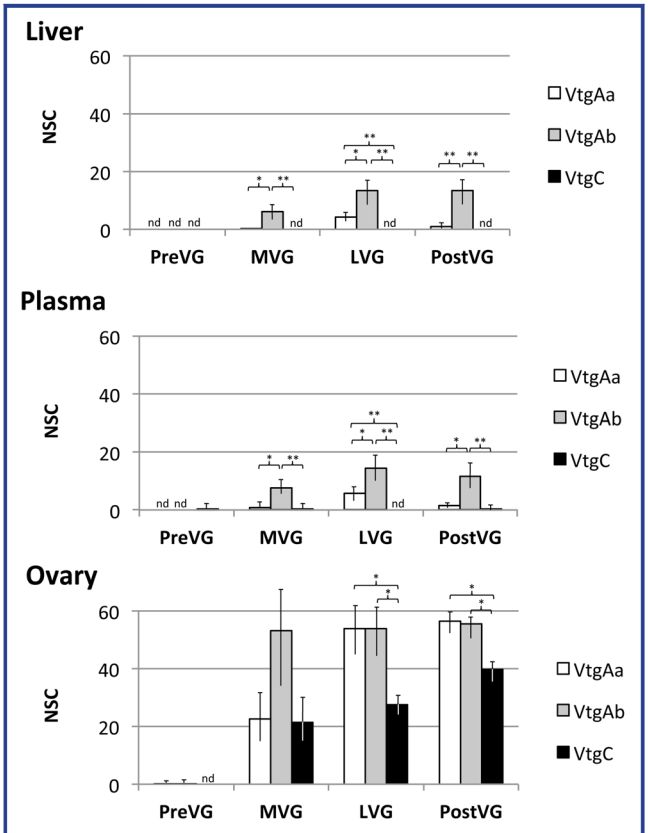

Figure 1. Normalized spectral counts (NSC) for vitellogenin (VtgAa, VtgAb, and VtgC) proteins detected in striped bass liver, plasma, and ovary during PreVG, MVG, LVG, and PostVG. Significant differences detected by one-way ANOVA followed by a post hoc Tukey–Kramer Honestly Significant Difference (HSD) test for comparisons of mean transformed NSC values for Vtgs by type within tissues are denoted by the horizontal brackets and asterisks as follows: $^{*}P \leq 0.05$ and $^{**}P \leq 0.005$. Samples for which vitellogenin proteins were not detected by the instrument are denoted by "nd." ANOVA, analysis of variance; LVG, late-vitellogenesis; MVG, mid-vitellogenesis; NSC, normalized spectral counts; nd, not detected; PreVG, pre-vitellogenesis; PostVG, post-vitellogenesis; HSD, Tukey–Kramer Honestly Significant Difference; VtgAa, VtgAb, and VtgC, vitellogenins.

four ovarian stages was calculated as the ratio of their NSC values and is reported in Table 1 and graphically represented in Figure 2. The proportional abundance of each Vtg by sample type was also calculated for each ovarian stage as a ratio of the respective NSC values (liver/plasma/ovary). Based upon these calculations, the Vtg ratios changed in each tissue type throughout vitellogenesis and the ovary generally contained substantially more YPAa, YPAb, and YPC than the plasma or liver.

Polyacrylamide Gel Electrophoresis (SDS–PAGE) and Western Blotting

Vitellogenin-type-specific polyclonal antisera raised against gray mullet Lvs (α-Mullet LvAa, α-Mullet LvAb, and α-Mullet LvC) specifically recognized the corresponding purified white perch Vtg (Fig. 3) and Western blots using these antisera clearly revealed the presence of three forms of immunologically distinct Vtg or Vtg-derived protein in the liver, plasma, and ovary of striped bass (Fig. 4). The VtgAa was resolved as a 120 kDa protein with 95 and 97 kDa degradation products in the striped bass liver that intensely stained during PreVG, however the immunoreactivity declined by MVG. The VtgAb was faintly detected in striped bass liver as 120 and 95 kDa proteins during PreVG and the staining intensity declined during MVG, however it increased during PostVG. The VtgAa and VtgAb were detected in plasma as 183 and 184 kDa proteins, respectively, from PreVG through LVG. The VtgC exhibited comparatively lower immunoreactivity in all the blots and was barely detectable in female plasma and liver. Derivative YPs corresponding to all three Vtg-types were detected in the MVG ovary and these YPs reached maximum staining intensity by PostVG. The three YPs in the ovary with molecular weights of 114, 116, and 111 kDa are identified as striped bass LvHAa, LvHAb, and LvHC, respectively (Hiramatsu et al., 2002a; Williams et al., 2014). Numerous, immunoreactive YPs of lower molecular weight (23–102 kDa) corresponding to all three Vtg-types also were present in the ovary from MVG to PostVG. Negative control male plasma exhibited no immunoreactivity with the antisera, whereas proteins corresponding to the appropriate sizes of each Vtg-type were detected in the positive control from E_2-induced males.

Semi-Quantitative Reverse Transcription Polymerase Chain Reaction (RT-PCR)

The primary site of transcription of all three striped bass *vtgs* during MVG is the liver (Fig. 5). This is apparent by cycles 30–35 of the RT-PCR when the housekeeping gene (*rpl9*) product reaches maximum amplification. Secondary sites of *vtgAa* transcription are the ovary and foregut. Weak expression of all three *vtgs* is detected by 35 cycles in brain, adipose, muscle, and heart.

Real-Time Quantitative RT-PCR

Absolute quantitative expression of *vtgAa*, *vtgAb*, and *vtgC* transcripts in striped bass liver and ovary during PreVG, MVG, LVG, and PostVG was assessed by real-time quantitative RT-PCR and the results are shown in Figures 6 and 7, respectively. During MVG, LVG, and PostVG, levels of *vtgAb* transcripts in liver were significantly higher than those for *vtgC*. The *vtgAa* had the highest expression in ovary during PreVG, MVG, and PostVG. Although all three *vtg* transcripts were detected in liver and ovary during PreVG, this extra-hepatic *vtg* gene expression was considered to result in only trace levels of the transcripts because their levels in liver during MVG through PostVG were, on average, at least 1,200-fold greater.

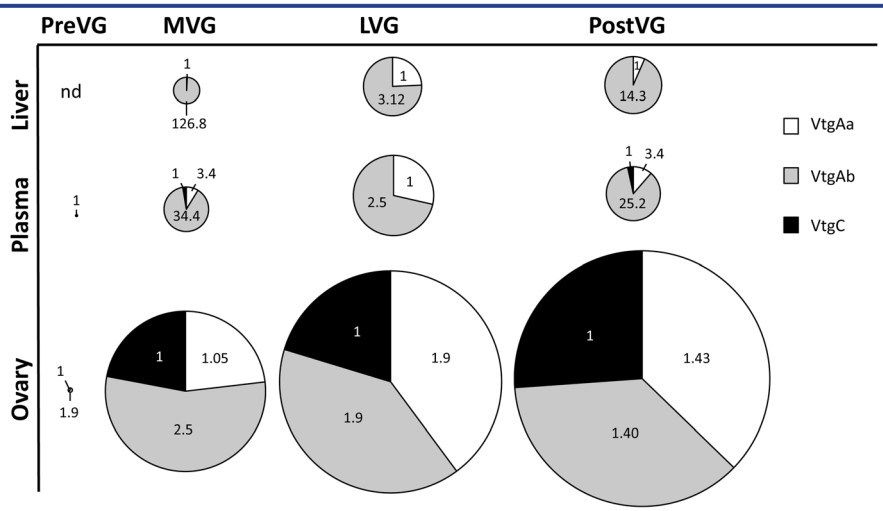

Figure 2. Proportional representation of vitellogenins (VtgAa, VtgAb, and VtgC) based on ratios of their normalized spectral counts (NSC) in striped bass liver, plasma, and ovary during PreVG, MVG, LVG, and PostVG. The radius of each pie chart is based on the sum of all NSC values for all three vitellogenins in each sample type and time. Numbers associated with each partition indicate the relative abundance of proteins derived from each vitellogenin type, with the lowest abundance set to 1. Samples for which vitellogenin proteins not detected by the instrument are denoted by "nd." LVG, late-vitellogenesis; MVG, mid-vitellogenesis; NSC, normalized spectral counts; nd, not detected; PreVG, pre-vitellogenesis; PostVG, post-vitellogenesis; VtgAa, VtgAb, and VtgC, vitellogenins.

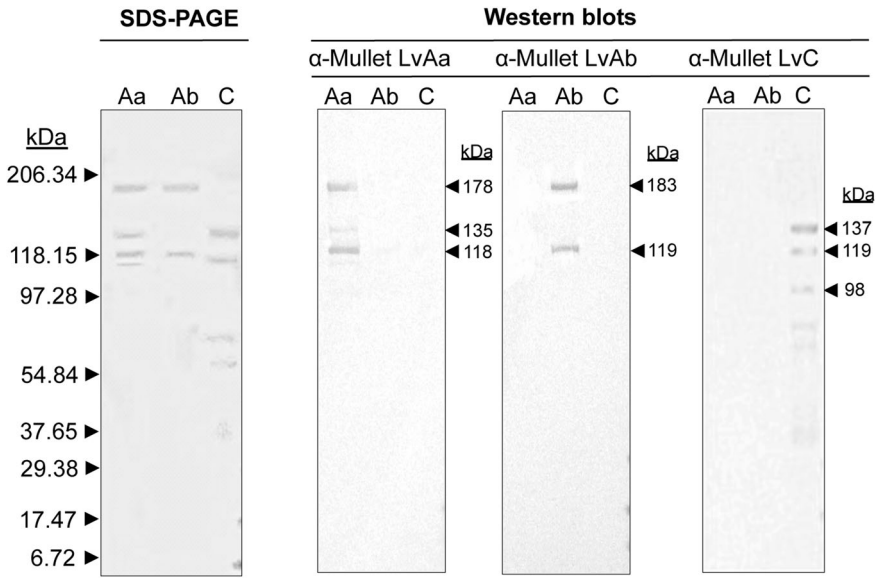

Figure 3. SDS–PAGE gel stained with Coomassie brilliant blue and corresponding Western blots using antilipovitellin Aa (α-Mullet LvAa), Ab (α-Mullet LvAb), and C (α-Mullet LvC) from gray mullet. These antisera are described in Amano et al. (2007a, b, 2008). Gel lanes are indicated as follows: Aa, purified white perch VtgAa; Ab, purified white perch VtgAb; C, purified white perch VtgC. Numbers and associated arrows to the left of the SDS–PAGE gel indicate the sizes and positions of molecular weight markers (kDa). Numbers and associated arrows to the right of the Western blots indicate the positions and sizes of immunoreactive vitellogenin proteins. Aa, purified white perch VtgAa; Ab, purified white perch VtgAb; α-Mullet LvAa, antilipovitellin Aa from gray mullet; α-Mullet LvAb, antilipovitellin Ab from gray mullet; α-Mullet LvC, antilipovitellin C from gray mullet; C, purified white perch VtgC; kDa, kilodaltons; SDS–PAGE, sodium dodecyl sulfate–polyacrylamide gel electrophoresis.

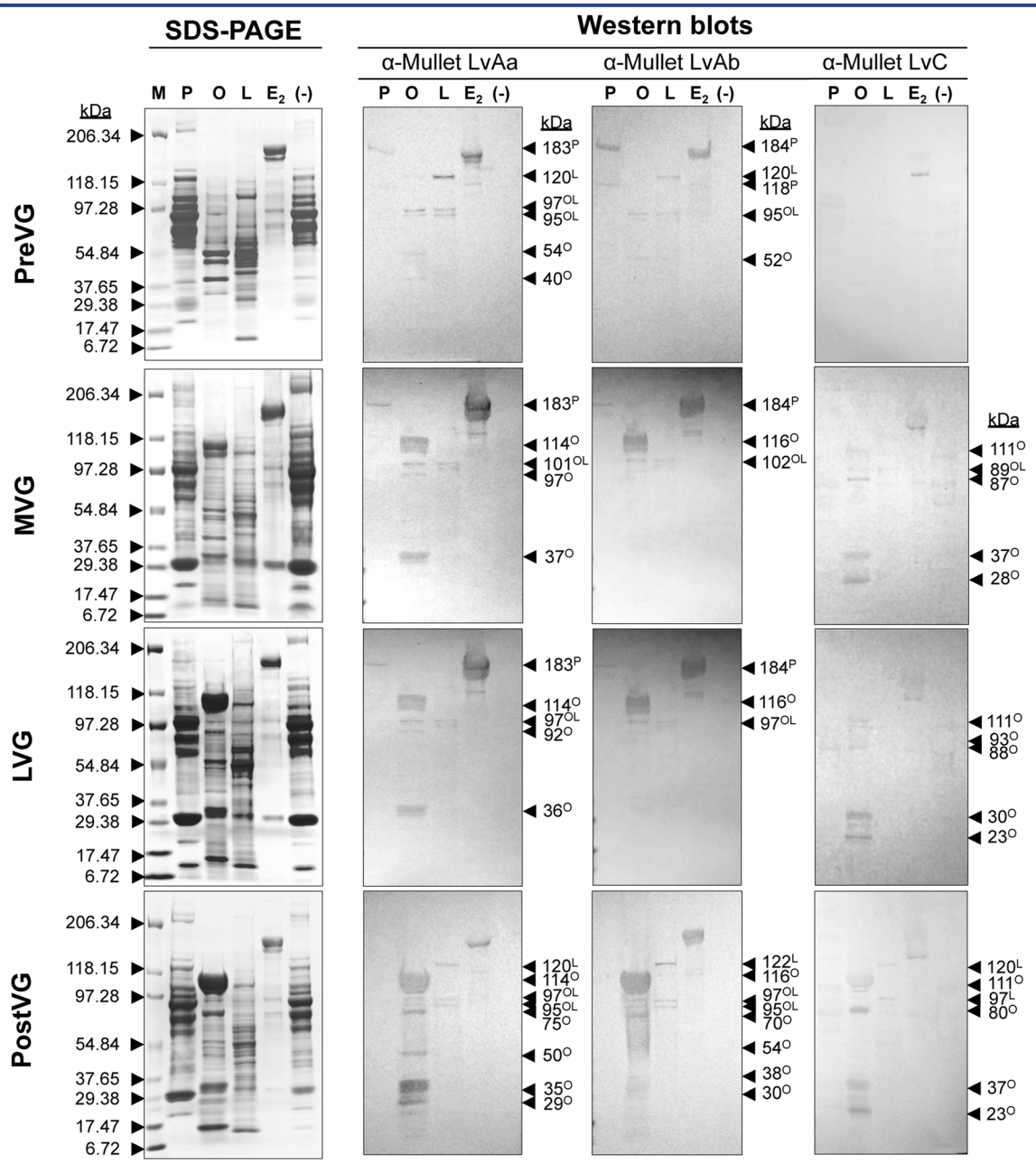

Figure 4. SDS–PAGE stained with Coomassie brilliant blue and Western blots using antilipovitellin Aa (α-Mullet LvAa), Ab (α-Mullet LvAb), and C (α-Mullet LvC) from gray mullet. Gel lanes are indicated as follows: striped bass plasma (P), ovary (O), liver (L), estrogen-induced male plasma (E_2), and male control plasma (–). Gels and blots are indicated as follows: PreVG, MVG, LVG, and PostVG. Numbers and associated arrows to the left of the SDS–PAGE gel indicate the sizes and positions of molecular weight markers (kDa). Numbers and associated arrows to the right of the Western blots indicate the positions and sizes of immunoreactive vitellogenin-derived proteins in P, O, and L samples. α-Mullet LvAa, antilipovitellin Aa from gray mullet; α-Mullet LvAb, antilipovitellin Ab from gray mullet; α-Mullet LvC, antilipovitellin C from gray mullet; E_2, estrogen-induced male plasma; kDa, kilodaltons; LVG, late-vitellogenesis; L, liver; (–), male control plasma; MVG, mid-vitellogenesis; O, ovary; P, plasma; PostVG, post-vitellogenesis; PreVG, pre-vitellogenesis; SDS–PAGE, sodium dodecyl sulfate–polyacrylamide gel electrophoresis.

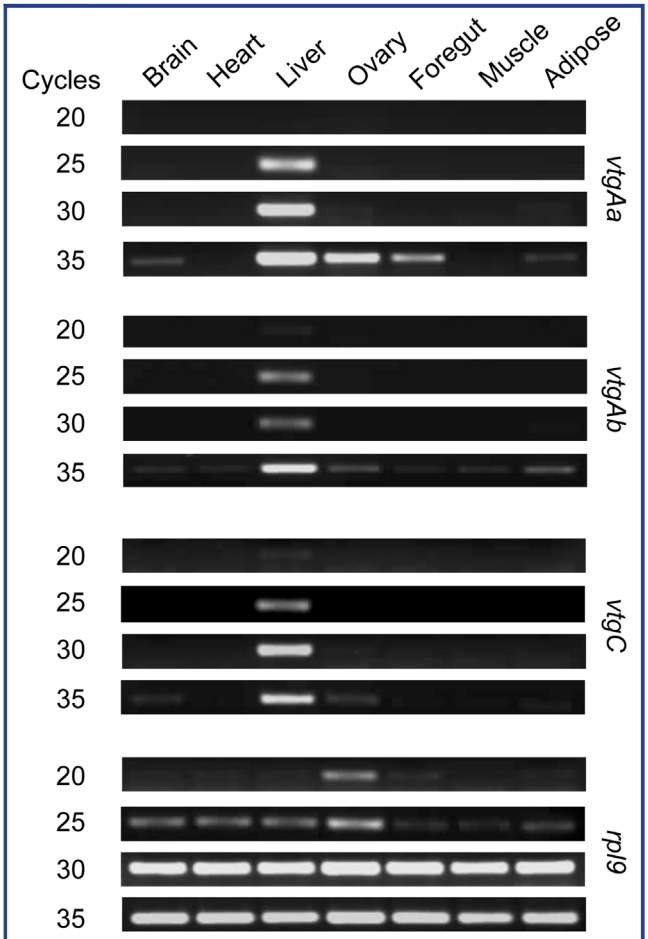

Figure 5. Results of semi-quantitative reverse transcription polymerase chain reaction (RT-PCR) used to visualize the relative abundance of gene transcripts corresponding to vitellogenin Aa (*vtgAa*), vitellogenin Ab (*vtgAb*), vitellogenin C (*vtgC*), and ribosomal protein L9 (*rpl9*) in various tissues obtained from female striped bass at mid-vitellogenesis. Cycle numbers for each RT-PCR are indicated to the left of the gels. *rpl9*, ribosomal protein L9; RT-PCR, semi-quantitative reverse transcription polymerase chain reaction; *vtgAa*, *vtgAb*, and *vtgC*, *vitellogenins*.

Relative quantitative expression of *vtgAa*, *vtgAb*, and *vtgC* transcripts in striped bass liver during PreVG, MVG, LVG, and PostVG was assessed by real-time quantitative RT-PCR and the results are shown in Figure 8. The liver expression of the internal reference gene (*rpl9*) did not significantly change across ovarian stage (average fold-change 1.6 ± 1.0 standard error of the mean). Expression of *vtgAb* in the liver significantly increased from PreVG to MVG ($P = 0.005$), PreVG to LVG ($P = 0.0002$), and PreVG to PostVG ($P = 0.0002$), MVG to LVG ($P = 0.0386$), and MVG to PostVG ($P = 0.0312$). Expression of *vtgAa* in liver significantly increased from PreVG to MVG ($P = 0.022$), PreVG to LVG ($P = 0.0004$), PreVG to PostVG ($P = 0.0005$), MVG to LVG ($P = 0.017$), and MVG to PostVG ($P = 0.0218$). The expression of *vtgC* in liver significantly increased from PreVG to LVG ($P = 0.0331$) and PreVG to PostVG ($P = 0.0075$).

DISCUSSION

In this study, we report on quantitative measurement by MS and spectral counting of three distinct types of Vtg protein in the liver, plasma, and ovary of female striped bass sampled at four key stages of their annual reproductive cycle. Western blots using Vtg-type-specific polyclonal antisera raised against the corresponding gray mullet Lvs were used to confirm these findings. Additionally, we evaluated expression of the three *vtg* gene transcripts in several different tissues of female striped bass.

After rigorous purification, the Lvs derived from gray mullet VtgAa, VtgAb, and VtgC were utilized as antigens to create rabbit antisera (α-Mullet LvAa, α- Mullet LvAb, and α- Mullet LvC) that specifically recognize the respective mullet Lv or parent Vtg (Amano et al., 2007a), and these antisera were employed in the present study to detect the three striped bass Vtgs and their protein products in plasma, liver and ovary (Fig. 4). Western blotting of purified white perch VtgAa, VtgAb, and VtgC confirmed the specificity of each of these antisera for the respective *Moronidae* Vtg (Fig. 3), each of which is nearly identical between white perch and striped bass (96–99% amino acid identity) (Reading et al., 2009; Williams et al., 2014). Maximal accumulation of Vtg proteins by the striped bass ovary occurs by PostVG, just prior to ovulation. This is evidenced by the intensity of immunoreactive staining of 114, 116, and 111 kDa proteins corresponding to LvHAa, LvHAb, and LvHC, respectively (Fig. 4) and by the results of the MS and spectral counting procedures (Table 1 and Fig. 1). The other immunoreactive proteins of lower molecular weight in the ovary represent Vtg-derived YPs that result from proteolytic processing prior to their storage in the yolk (Williams et al., 2014).

The profiles of Vtg accumulation by the growing oocytes over different stages of oogenesis differed by Vtg type (Table 1, Figs. 1 and 2). Although trace levels of VtgAb-derived YPs were detected in the ovary during PreVG, appreciable accumulation was not evident until MVG, and this accumulation continued until PostVG. In contrast, VtgAa began to enter the oocyte during MVG, with a substantial increase in rates of uptake by LVG, during which time the level of VtgAa proteins becomes equal to that of VtgAb proteins in the ovary. The VtgC appears to be steadily accumulated by oocytes from MVG through PostVG, contributing to a significantly lower proportion of total Vtg-derived YP as compared to VtgAa and VtgAb.

Both VtgAa and VtgAb were detected by Western blotting from PreVG through MVG in the plasma as 183 and 184 kDa proteins, respectively (Fig. 4). These molecular weights are consistent with the sizes of the complete type-Vtg monomers in striped bass (Williams et al., 2014). The VtgC, however was not detected in plasma by Western blotting during any ovarian stage, yet was

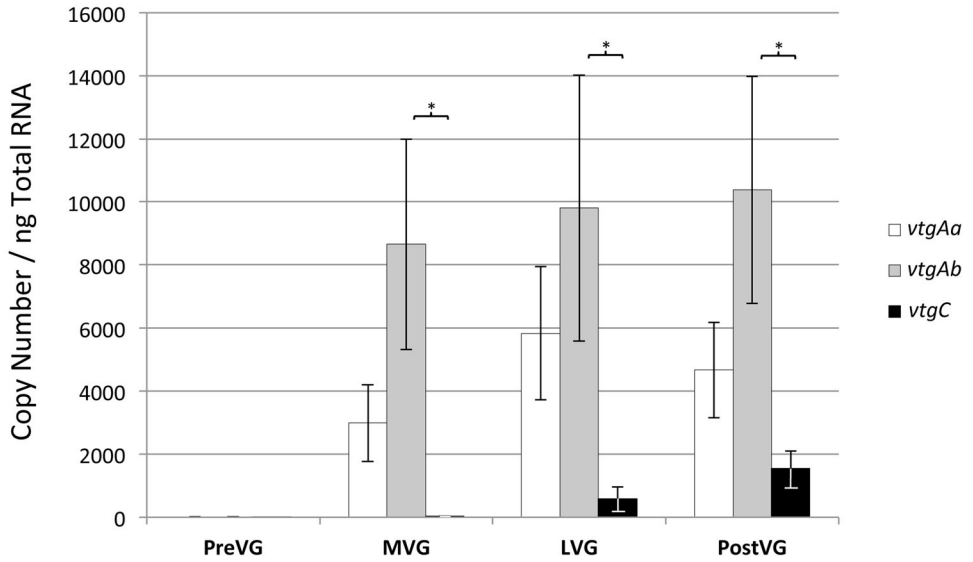

Figure 6. Results of absolute quantitative real-time RT-PCR used to quantify vitellogenin gene (*vtgAa*, *vtgAb*, and *vtgC*) transcripts present in striped bass liver during PreVG, MVG, LVG, and PostVG. Significant differences detected by one-way ANOVA followed by a post hoc Tukey–Kramer Honestly Significant Difference (HSD) test for comparisons of values for *vtgs* by type within a stage of vitellogenesis are denoted by the horizontal brackets and asterisks as follows: $^{*}P \leq 0.05$ and $^{**}P \leq 0.005$. Vertical lines represent the standard error of the mean (N = three). ANOVA, analysis of variance; LVG, late-vitellogenesis; MVG, mid-vitellogenesis; PCR, polymerase chain reaction; PostVG, post-vitellogenesis; PreVG, pre-vitellogenesis; HSD, Tukey–Kramer Honestly Significant Difference; *vtgAa*, *vtgAb*, and *vtgC*, *vitellogenins*.

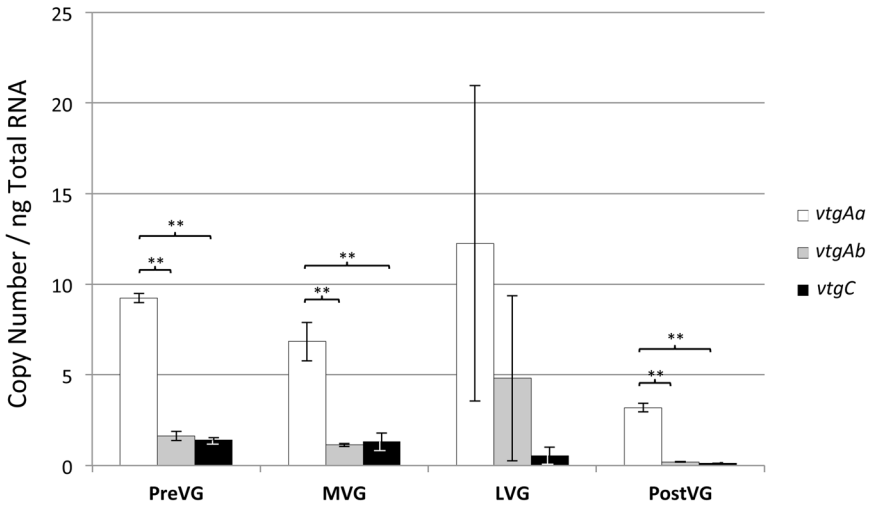

Figure 7. Results of absolute quantitative real-time RT-PCR used to quantify vitellogenin gene (*vtgAa*, *vtgAb*, and *vtgC*) transcripts present in striped bass ovary during PreVG, MVG, LVG, and PostVG. Significant differences detected by one-way ANOVA followed by a post hoc Tukey–Kramer Honestly Significant Difference (HSD) test for comparisons of values for *vtgs* by type within a stage of vitellogenesis are denoted by the horizontal brackets and asterisks as follows: $^{*}P \leq 0.05$ and $^{**}P \leq 0.005$. Vertical lines represent the standard error of the mean (N = three). ANOVA, analysis of variance; LVG, late-vitellogenesis; MVG, mid-vitellogenesis; PCR, polymerase chain reaction; PostVG, post-vitellogenesis; PreVG, pre-vitellogenesis; HSD, Tukey–Kramer Honestly Significant Difference; *vtgAa*, *vtgAb*, and *vtgC*, *vitellogenins*.

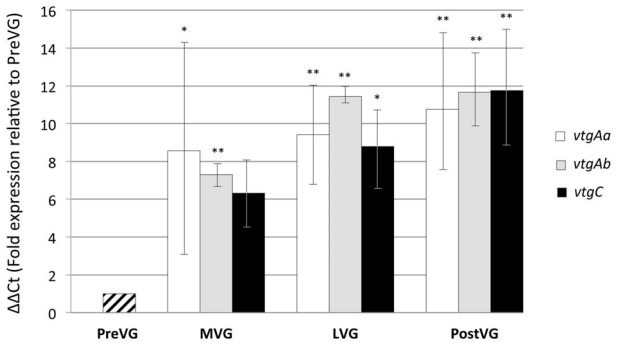

Figure 8. Results of relative quantitative real-time RT-PCR used to quantify vitellogenin gene (*vtgAa*, *vtgAb*, and *vtgC*) transcripts present in striped bass liver during PreVG, MVG, LVG, and PostVG. Data are shown as expression (fold) relative to that of each respective *vtg* type during PreVG. Significant differences detected by one-way ANOVA followed by a post hoc Tukey–Kramer Honestly Significant Difference (HSD) test are denoted by the asterisks as follows: $^{*}P \leq 0.05$ and $^{**}P \leq 0.005$. Vertical lines represent the standard error of the mean ($N =$ three). ANOVA, analysis of variance; LVG, late-vitellogenesis; MVG, mid-vitellogenesis; PCR, polymerase chain reaction; PostVG, post-vitellogenesis; PreVG, pre-vitellogenesis; HSD; Tukey–Kramer Honestly Significant Difference; *vtgAa*, *vtgAb*, and *vtgC*, *vitellogenins*.

detected at trace levels by MS and spectral counting during PreVG, MVG, and PostVG (Table 1, Fig. 1). Neither VtgAa nor VtgAb were detected in plasma during PreVG by the MS procedure, but the levels (NSC) of these Vtgs increased from MVG through LVG, consistent with the time frame of their maximal uptake by the ovary (Figs. 1 and 2). Plasma VtgAa and VtgAb then declined during PostVG. As assessed by MS and spectral counting, the VtgAb predominates in the plasma from MVG through PostVG.

The VtgAa and VtgAb were detected in the liver at all ovarian stages by Western blotting as 95–120 kDa proteins (Fig. 4). The reason for this difference in apparent mass of VtgAa and VtgAb between plasma and liver is unclear, but it may relate to proteolytic degradation during post mortem processing of the liver tissue. The VtgAa and VtgAb are labile and prone to degradation by endogenous enzymes (Tao et al., '93), which could explain their lower apparent molecular weight in the liver sample. As assessed by MS and spectral counting, the VtgAb was predominant in liver during MVG and PostVG, and both VtgAa and VtgAb were significantly higher than VtgC in liver during LVG and PostVG (Figs. 1 and 2). The *vtgAb* also exhibited highest expression in liver during MVG, LVG and PostVG, however the average *vtgAb* transcript levels were only significantly higher than those of *vtgC* (Fig. 6). When hepatic transcript levels for the same three *vtgs* were measured in E_2-treated male tilapia, *vtgAb* transcripts were similarly more abundant than *vtgC* (Davis et al., 2007).

The VtgC exhibited comparatively lower immunoreactivity in all Western blots (Fig. 4) and was not detected in female liver by MS and spectral counting at any ovarian stage (Figs. 1 and 2). Explanations of this observation include the possibilities that levels of VtgC protein in the liver is below the MS detection threshold or that the liver rapidly exports VtgC into the plasma following its synthesis. Similarly, the VtgAa and VtgAb were not detected by MS and spectral counting, or were present at only trace levels, in the PreVG liver, plasma, and ovary, therefore Western blotting may be more sensitive for detecting low levels of Vtgs as compared to the MS procedure. The *vtgC* also had the lowest level of hepatic expression among the three *vtgs*, as evidenced by the results of real-time RT-PCR. Alternatively, since Vtgs and YPs tend to form precipitates or aggregates (Amano et al., 2007a), the different solutions used during extraction of these proteins from the plasma or tissues samples may have resulted in the inconsistent results between the Western blotting and MS procedures. For example, some of the Vtg or YP components may not have been very soluble in water and, hence, would not be efficiently extracted from the samples for detection by MS.

Despite our inability to detect VtgC protein in liver by Western blotting or by MS and spectral counting, semi-quantitative RT-PCR confirmed that the liver is the predominant site of *vtgC* expression (Fig. 5). Therefore, extra-hepatic production of VtgC is unlikely to significantly contribute to vitellogenesis in striped bass. Perhaps of interest in this regard is the expression of *vtgAa* in the ovary and foregut, which suggests that extra-hepatic production of VtgAa might contribute to vitellogenesis. Extra-hepatic production of *vtgs* has been reported in zebrafish and rainbow trout (*Oncorhynchus mykiss*; Wang et al., 2005; Levi et al., 2012; Tingaud-Sequeira et al., 2012), but the biological significance of these observations is unclear with respect to the present study as expression of *vtgs* in striped bass ovary is miniscule in comparison to liver (Figs. 6 and 7). Further investigation will be required to confirm the importance of the "ectopic" expression of *vtg* transcripts, however it is apparent that the liver is the primary site of expression for all three *vtgs* in the striped bass.

Typically in the *Moronidae* species, levels of circulating Vtg have been reported to be sustained at or near maximum values during the latter half of vitellogenesis, which corresponds approximately to the period from MVG to PostVG in the present study (Tao et al., '93; Blythe et al., '94; Berlinsky et al., '95; Jackson and Sullivan, '95; Heppell et al., '99; Clark et al., 2005). Although VtgAa and VtgAb must concurrently enter the oocyte to some extent throughout vitellogenesis (Figs. 1 and 2), the primary periods of uptake by the oocyte of these two types of Vtg differ. The VtgAb is always the predominant form of Vtg in the plasma, reaching peak levels at LVG, and is the dominant form of Vtg contributing to yolk formation up until MVG. In contrast, although the VtgAa also reaches peak levels in the plasma by

LVG, the subsequent rate of VtgAa accumulation in the ovary after MVG far surpasses that of VtgAb, despite the substantially higher plasma levels of VtgAb during this time. Therefore, the oocyte accumulates VtgAb most substantially up until MVG and preferentially accumulates VtgAa thereafter, and these processes are not necessarily dependent on the prevailing plasma Vtg concentrations.

Based on the quantitative differences and temporal changes in plasma and ovarian levels of VtgAa, VtgAb, and VtgC proteins, we propose a new tripartite model of vitellogenesis in striped bass, which is depicted in Figure 9. In this model, VtgAb enters the oocytes primarily during the earlier phases of vitellogenesis, uptake of VtgAa by the oocytes is mainly relegated to the latter half of vitellogenesis, and uptake of VtgC by the oocytes proceeds

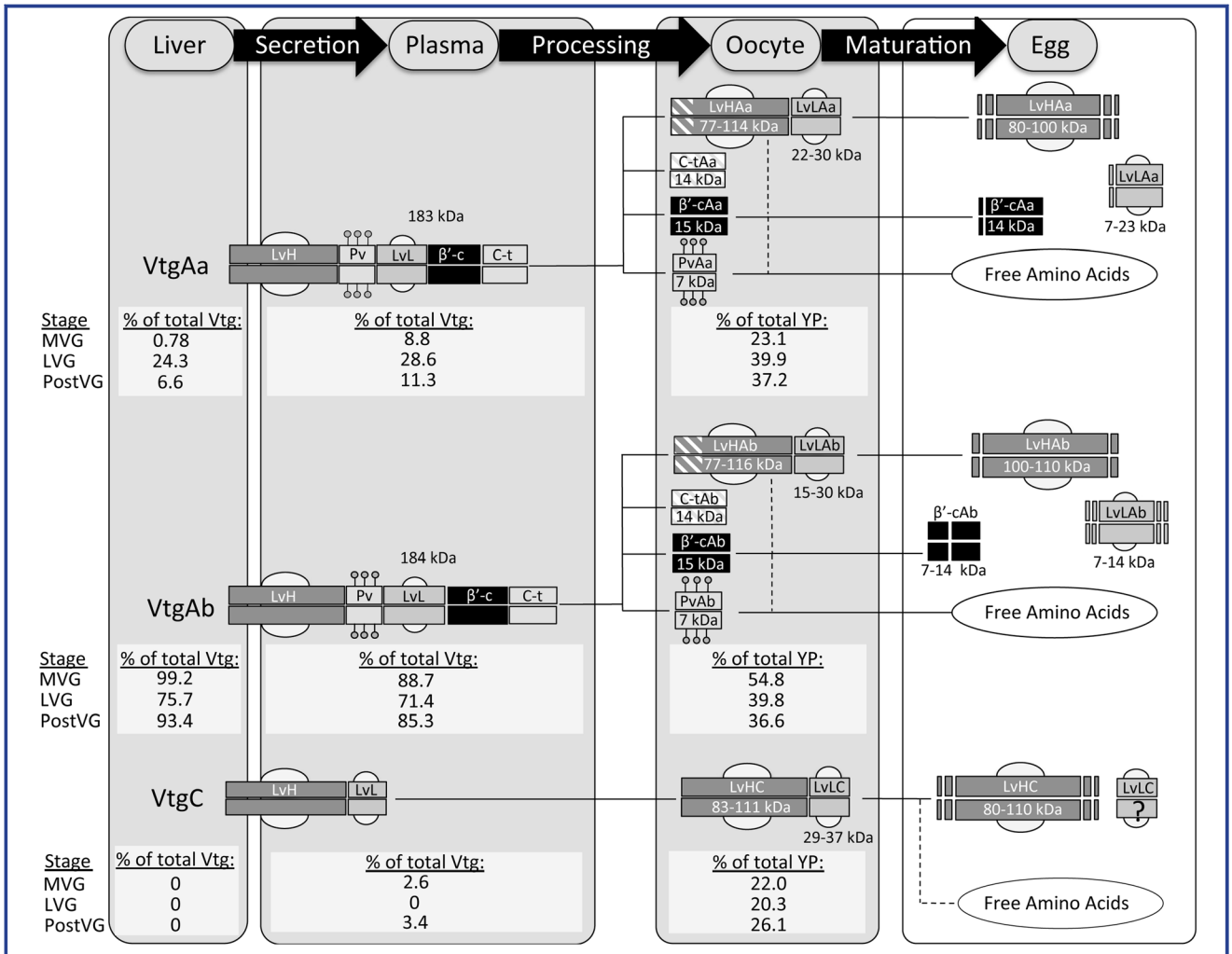

Figure 9. Model depicting molecular alterations of the three types of vitellogenins (VtgAa, VtgAb, and VtgC) during vitellogenesis (Secretion and Processing) and oocyte cytoplasmic maturation (Maturation) in striped bass. Structures of Vtgs and their product yolk proteins (lipovitellin heavy chain, LvH; phosvitin, Pv; lipovitellin light chain, LvL; beta-component, β′-c; and C-terminal domain, C-t) in liver, plasma, oocytes, and ovulated eggs are shown. The percentage of total Vtg protein comprised by VtgAa, VtgAb, and VtgC in liver, plasma, and ovary of each form of Vtg during MVG, LVG, and PostVG is also indicated (% of total Vtg or YP). The C-t and amino terminal portions of some LvHs derived from VtgAa and VtgAb are cleaved following uptake by the oocyte and these are indicated by the diagonal white bars. Although processing of LvHC and LvLC is evident following uptake by the oocyte, the presence of LvLC in the ovulated egg has not yet been verified and this is indicated by the "?." See Discussion section for details (see also: Williams et al., 2014). β′-c, beta-component; C-t, C-terminal domain; LVG, late-vitellogenesis; LvH, lipovitellin heavy chain; LvL, lipovitellin light chain; MVG, mid-vitellogenesis; Pv, phosvitin; PostVG, post-vitellogenesis; VtgAa, VtgAb, and VtgC, vitellogenins; YP, yolk proteins.

steadily throughout vitellogenesis. This model also incorporates recent findings on the processing of Vtg-derived YPs in striped bass that are reported in Williams et al. (2014). The disparate accumulation of different forms of Vtg by the growing fish oocyte appears to be precisely regulated both by rates of hepatic synthesis and secretion leading to their availability in plasma and, ultimately, interstitial fluid and by mechanisms for receptor-mediated uptake of the Vtg into the ooplasm (Sawaguchi et al., 2008). A system of dual and specific Vtgrs would provide oocytes with a mechanism to regulate the proportional accumulation of VtgAa and VtgAb in the yolk (Reading et al., 2011; Hiramatsu et al., 2013). In the white perch, VtgC does not bind to preparations of ovary membrane proteins and, therefore, it may nonspecifically enter the oocyte in the fluid phase of endocytosis (Reading et al., 2011). We observed steady accumulation of VtgC by the striped bass ovary at comparatively lower levels than that of VtgAa and VtgAb, further supporting this possibility for the temperate basses (Genus *Morone*).

The proportional abundance of different forms of Vtg in tissues involved in vitellogenesis has been reported for barfin flounder (Sawaguchi et al., 2008) and gray mullet (Amano et al., 2008). The proportional abundance of VtgAa/VtgAb/VtgC in plasma of striped bass during MVG (3:34:1) and PostVG (3:25:1) is different from that reported for barfin flounder (13:18:1 and 32:10:1, respectively), such that VtgAa makes up a greater proportion of the plasma Vtgs in barfin flounder as compared to striped bass. The abundances of YPs derived from VtgAa and VtgAb are equivalent in the LVG striped bass ovary, whereas YPAb predominates the yolk of vitellogenic gray mullet, with the proportional abundance of YPAa/YPAb/YPC being 4:13.3:1 (Amano et al., 2008). Therefore, different species of fishes may have different rates of hepatic production of the various forms of Vtg relative to rates of uptake of these Vtgs into growing oocytes during vitellogenesis.

The proportion of VtgAa/VtgAb/VtgC accumulated in the PostVG ovary of striped bass (1.4:1.4:1) and of barfin flounder (9:15:1), expressed as percentages, also differ. In both species, VtgAa comprises 36% of the total YP, however VtgAb comprises 60% of the remaining YP in barfin flounder (Sawaguchi et al., 2008; see also: Reading and Sullivan, 2011) as opposed to only 36% in striped bass due to the greater relative abundance of VtgC in this species (28% in striped bass compared to 4% in barfin flounder). The differences in yolk composition may relate to the unique life histories of these species, such as the time required for embryos to develop up until hatching or the time required from hatching to onset of exogenous feeding. Striped bass typically hatch 36–48 hr after fertilization at a water temperature of approximately 20°C, as compared to 8 days for barfin flounder (Du et al., 2010). Since YPC appears to serve as a nutrient source for late stage larvae (Sawaguchi et al., 2005b), abundant YPC reserves in the eggs of striped bass may relate to the observation that free-swimming yolk sac larvae can survive for a considerable amount of time after hatching in the absence of feeding (Eldridge, '81). As a final note, environmental salinities of the spawning habitats and specific gravities of the ovulated eggs also differ between these two species, and this also may relate to the Vtg composition of the yolk and eventual YP processing during ovarian maturation. For instance, barfin flounder spawn pelagic eggs in marine water, whereas striped bass spawn neutrally buoyant eggs in fresh water.

We have reported the relative quantification of three distinct Vtgs in liver, plasma, and ovary throughout the process of ovarian recrudescence in the striped bass. Our results show that growing ovarian follicles precisely and independently regulate the accumulation of multiple Vtgs by their rates of hepatic secretion and receptor-mediated uptake into the ooplasm. Furthermore, our results indicate that several aspects of this process may be species-specific among fishes, possibly relating to differences in their reproductive strategies. Additional information on the multiple Vtg-systems of other fishes will be required for further understanding of the complex and variable physiology of egg yolk formation and its relationship to successful and dysfunctional reproduction.

ACKNOWLEDGMENTS

We thank Dr. A. S. McGinty and M. S. Hopper from the NCSU PAFL and B. D. Ring from the NCSU Aquaculture Research Laboratory for rearing the experimental animals. We acknowledge A. L. Boury with assistance during sampling of experimental animals at the NCSU PAFL. We thank Dr. D. A. Baltzegar for assistance with real-time RT-PCR normalization.

LITERATURE CITED

Amano H, Fujita T, Hiramatsu N, et al. 2007a. Purification of mulitple vitellogenins in gray mullet (*Mugil cephalus*). Mar Biol 152:1215–1225.

Amano H, Fujita T, Hiramatsu N, et al. 2007b. Egg yolk proteins in gray mullet (*Mugil cephalus*): purification and classification of multiple lipovitellins and other vitellogenein-derived yolk proteins and molecular cloning of the parent vitellogenin genes. J Exp Zool 307A:324–341.

Amano H, Fujita T, Hiramatsu N, et al. 2008. Multiple vitellogenin-derived yolk proteins in gray mullet (*Mugil cephalus*): disparate proteolytic patterns associated with ovarian follicle maturation. Mol Reprod Dev 75:1307–1317.

Berlinsky DL, Specker JL. 1991. Changes in gonadal hormones during oocyte development in the striped bass, *Morone saxatilis*. Fish Physiol Biochem 9:51–62.

Berlinsky DL, Jackson LF, Sullivan CV. 1995. The annual reproductive cycle of white bass, *Morone chrysops*. J World Aquacult Soc 26:252–260.

Blythe WG, Helfrich LA, Sullivan CV. 1994. Sex steroid hormone and vitellogenin levels in striped bass (*Morone saxatilis*) maturing under 6-, 9-, and 12-month photothermal cycles. Gen Comp Endocrinol 94:122–134.

Clark RW, Henderson-Arzapalo A, Sullivan CV. 2005. Disparate effects of annually-cycling daylength and water temperature on reproductive maturation of striped bass (*Morone saxatilis*). Aquaculture 249:497–513.

Davis LK, Hiramatsu N, Hiramatsu K, et al. 2007. Induction of three vitellogenins by 17beta-estradiol with concurrent inhibition of the growth hormone-insulin-like growth factor-I axis in a euryhaline teleost, the tilapia (*Oreochormis mossambicus*). Biol Reprod 77:614–625.

Du R, Wang Y, Jiang H, et al. 2010. Embryonic and larval development in barfin flounder (*Verasper moseri*) (Jordan and Gilbert). Chin J Ocean Limnol 28:18–25.

Eldridge MB. 1981. Effects of food and feeding factors on laboratory-reared striped bass larvae. Trans Am Fish Soc 110:111–120.

Finn RN. 2007a. The maturational disassembly and differential proteolysis of paralogous vitellogenins in a marine pelagophil teleost: a conserved mechanism of oocyte hydration. Biol Reprod 76:936–948.

Finn RN. 2007b. Vertebrate yolk complexes and the functional implications of phosvitins and other subdomains in vitellogenins. Biol Reprod 76:926–935.

Finn RN, Kristofferson BA. 2007. Vertebrate vitellogenin gene duplication in relation to the "3R Hypothesis": correlation to the pelagic egg and the oceanic radiation of teleosts. PLoS ONE 2:e169.

Geist J, Werner I, Eder KJ, Leutenegger CM. 2007. Comparison of tissue-specific transcription of stress response genes with whole animal endpoints of adverse effect in striped bass (*Morone saxatilis*) following treatment with copper and esfenvalerate. Aquat Toxicol 85:28–39.

Heppell SA, Jackson LF, Weber GM, Sullivan CV. 1999. Enzyme-linked immunosorbent assay (ELISA) of vitellogenin in temperate basses (Genus *Morone*): plasma and in vitro analyses. Trans Am Fish Soc 128:532–541.

Hiramatsu N, Hara A, Hiramatsu K, et al. 2002a. Vitellogenin-derived yolk proteins of white perch, *Morone americana*: purification, characterization and vitellogenin-receptor binding. Biol Reprod 67:655–667.

Hiramatsu N, Matsubara T, Hara A, et al. 2002b. Identification, purification and classification of multiple forms of vitellogenin from white perch (*Morone americana*). Fish Physiol Biochem 26:355–370.

Hiramatsu N, Cheek AO, Sullivan CV, Matsubara T, Hara A. 2005. Vitellogenesis and endocrine disruption. Biochem Mol Biol Fishes 6:431–471.

Hiramatsu N, Matsubara T, Fujita T, Sullivan CV, Hara A. 2006. Multiple piscine vitellogenins: biomarkers of fish exposure to estrogenic endocrine disrupters in aquatic environments. Mar Biol 149:35–47.

Hiramatsu N, Luo W, Reading BJ, et al. 2013. Multiple ovarian lipoprotein receptors in teleosts. Fish Physiol Biochem 39:29–32.

Jackson LF, Sullivan CV. 1995. Reproduction of white perch (*Morone americana*): the annual gametogenic cycle. Trans Am Fish Soc 124:563–577.

Jonge HJM, Fehrmann RSN, de Bont ESJM, Hofstra RMW, Gerbens F. 2007. Evidence based selection of housekeeping genes. PLoS ONE 2: e898

Kolarevic J, Nerland A, Nilsen F, Finn RN. 2008. Goldsinny wrasse (*Ctenolabrus rupestris*) is an extreme vtgAa-type pelagophil teleost. Mol Reprod Dev 75:1011–1020.

Laemmli UK. 1970. Cleavage of structural proteins during the assembly of the head of bacteriophage T4. Nature 227:680–685.

LaFleur GJ, Byrne BM, Kanugo J, et al. 1995. *Fundulus heteroclitus* vitellogenin: the deduced primary structure of a piscine precursor to noncrystalline, liquid-phase yolk protein. J Mol Evol 41:505–521.

LaFleur GJ, Raldua D, Fabra M, et al. 2005. Derivation of major yolk proteins from parental vitellogenins and alternative processing during oocyte maturation in *Fundulus herteroclitus*. Biol Reprod 73:815–824.

Levi L, Ziv T, Admon A, Levavi-Sivan B, Lubzens E. 2012. Insight into molecular pathways of retinal metabolism, associated with vitellogenesis in zebrafish. Am J Physiol Endocrinol Metab 302: E626–E644.

Matsubara T, Ohkubo N, Andoh T, Sullivan CV, Hara A. 1999. Two forms of vitellogenin, yielding two distinct lipovitellins, play different roles during oocyte maturation and early development of barfin flounder, *Verasper moseri*, a marine teleost that spawns pelagic eggs. Dev Biol 213:18–32.

Nolan T, Hands RE, Bustin SA. 2006. Quantification of mRNA using real-time RT-PCR. Nat Protoc 1:1559–1582.

National Research Council. 1996. Guide for the care and use of laboratory animals. Washington, DC: National Academies Press.

Picha ME, Silverstein JT, Borski RJ. 2006. Discordant regulation of hepatic IGF-I mRNA and circulating IGF-I during compensatory growth in a teleost, the hybrid striped bass (*Morone chrysops* × *Morone saxatilis*). Gen Comp Endocrinol 147:196–205.

Reading BJ, Sullivan CV. 2011. Vitellogenesis in fishes. In: Ferrell AP, editor. Encyclopedia of fish physiology: from genome to environment. Maryland Heights, MO: Academic Press, Inc. Chapter 257, p 2272.

Reading BJ, Hiramatsu N, Sawaguchi S, et al. 2009. Conserved and variant molecular and functional features of multiple egg yolk precursor proteins (vitellogenins) in white perch (*Morone americana*) and other teleosts. Mar Biotechnol 11:169–187.

Reading BJ, Hiramatsu N, Sullivan CV. 2011. Disparate binding of three types of vitellogenin to multiple forms of vitellogenin receptor in white perch. Biol Reprod 84:392–399.

Reading BJ, Chapman RW, Schaff JE, et al. 2012. An ovary transcriptome for all maturational stages of the striped bass (*Morone saxatilis*), a highly advanced perciform fish. BMC Res Notes 5:111.

Reading BJ, Williams VN, Chapman RW, Williams TI, Sullivan CV. 2013. Dynamics of the striped bass (*Morone saxatilis*) ovary proteome reveal a complex network of the translasome. J Proteome Res 12:1691–1699.

Rees RA, Harrell RM. 1990. Artificial spawning and fry production of striped bass and hybrids. Culture and propagation of striped bass and its hybrids. Bethesda, MD: Striped Bass Committee, Southern Division, American Fisheries Society. p 43–72.

Reith M, Munholland J, Kelly J, Finn RN, Fyhn HJ. 2001. Lipovitellins derived from two forms of vitellogenin are differentially processed during oocyte maturation in haddock (*Melanogrammus aeglefinus*). J Exp Zool 291:58–67.

Sawaguchi S, Koya Y, Yoshizaki N, et al. 2005a. Multiple vitellogenins (vgs) in mosquitofish (*Gambusia affinis*): identification and characterization of three functional vg genes and their circulating and yolk protein products. Biol Reprod 72:1045–1060.

Sawaguchi S, Ohkubo N, Koya Y, Matsubara T. 2005b. Incorporation and utilization of multiple forms of vitellogenin and their derivative yolk proteins during vitellogenesis and embryonic development in the mosquitofish, *Gambusia affinis*. Zool Sci 22:701–710.

Sawaguchi S, Kagawa H, Ohkubo N, et al. 2006. Vitellogenin and their yolk protein products during oocyte growth and maturation in red seabream (*Pagrus major*), a marine teleost spawning pelagic eggs. Mol Reprod Dev 27:719–736.

Sawaguchi S, Ohkubo N, Amano H, et al. 2008. Controlled accumulation of multiple vitellogenins into oocytes during vitellogeneisis in the barfin flounder, *Verasper moseri*. Cybium Int J Ichthyol 32:262.

Tao Y, Hara A, Hodson RG, Woods LC, Sullivan CV III. 1993. Purification, characterization and immunoassay of striped bass (*Morone saxatilis*) vitellogenin. Fish Physiol Biochem 12:31–346.

Tingaud-Sequeira A, Knoll-Gellida A, André M, Babin PJ. 2012. Vitellogenin expression in white adipose tissue in female teleost fish. Biol Reprod 86:38.

Tipsmark CK, Baltzegar DA, Ozden O, Grubb BJ, Borski RJ. 2008. Salinity regulates claudin mRNA and protein expression in the teleost gill. Am J Physiol Regul Integr Comp Physiol 294:R1004–R1014.

Wang H, Yan T, Tan JTT, Gong Z. 2000. A zebra fish vitellogenin gene (vg3) encodes a novel vitellogenin without a phosvitin domain and may present a primitive vertebrate vitellogenin gene. Gene 256:303–310.

Wang H, Tan JTT, Emelyanov A, Korzh V, Gong Z. 2005. Hepatic and extrahepatic expression of vitellogenin genes in the zebrafish, *Danio rerio*. Gene 356:91–100.

Williams VN, Reading BJ, Hiramatsu N, et al. 2014. Multiple vitellogenins and product yolk proteins in striped bass, *Morone saxatilis*: molecular characterization and processing during oocyte growth and maturation. Fish Physiol Biochem 40:395–415.

Zhang Z, Wen Z, Washburn MP, Florens L. 2010. Refinements to label free proteome quantitation: how to deal with peptides shared by multiple proteins. Anal Chem 282:2272–2281.

Zybailov BL, Mosley AL, Sardiu ME, et al. 2006. Statistical analysis of membrane proteome expression changes in *Saccharomyces cerevisiae*. J Proteome Res 5:2339–2347.

Zybailov BL, Florens L, Washburn MP. 2007. Quantitative shotgun proteomics using a protease with broad specificity and normalized spectral abundance factors. Mol BioSyst 3:354–360.

SUPPORTING INFORMATION

Additional supporting information may be found in the online version of this article at the publisher's web-site.